Taylor & Francis
Taylor & Francis Group

Mitigating peak load and heat stress under heatwaves by optimizing adjustments of fan speed and thermostat setpoint

Zhujing Zhang, Kevin J. Kircher, Yuan Cai, Jonathon G. Brearley, David P. Birge & Leslie K. Norford

Published online: 24 Feb 2023.

Submit your article to this journal ↗

Article views: 1127

View related articles ↗

View Crossmark data ↗

Citing articles: 3 View citing articles ↗

Taylor & Francis
Taylor & Francis Group

🔓 OPEN ACCESS | Check for updates

Mitigating peak load and heat stress under heatwaves by optimizing adjustments of fan speed and thermostat setpoint

Zhujing Zhang[a], Kevin J. Kircher[b], Yuan Cai[a], Jonathon G. Brearley[a], David P. Birge[c] and Leslie K. Norford[a]

[a]Department of Architecture, Massachusetts Institute of Technology, Cambridge, MA, USA; [b]Department of Electrical Engineering and Computer Science, Massachusetts Institute of Technology, Cambridge, MA, USA; [c]Norman B. Leventhal Center for Advanced Urbanism, Massachusetts Institute of Technology, Cambridge, MA, USA

ABSTRACT

Heatwaves are becoming more frequent and severe, intensifying cooling demand and reducing air conditioner efficiencies. This causes peaks in electricity demand that pose operational challenges to power grids. This paper provides methods to mitigate demand peaks and heat stress under heatwaves by jointly adjusting fan speeds and thermostat setpoints in buildings. The methods involve (1) learning baseline models to predict load and thermal comfort, (2) fitting perturbation models that relate fan speed and thermostat setpoint adjustments to perturbations in load and thermal comfort, and (3) optimizing peak load and thermal comfort. The methods are implementable in real buildings, providing fast, accurately predicted optimized solutions that flatten demand peaks and mitigate personal heat stress. This paper demonstrates the methodology through simulation-based case studies of a single building and a six-building neighbourhood. In case studies, the methods reduce peak load by 8–10% while maintaining occupants' thermal comfort within safe and comfortable ranges.

Highlights

- This paper develops data-driven methods to reduce peak demand and mitigate heat stress during heatwaves.
- The methods are designed for straightforward implementation in the field.
- In case studies, the methods reduce peak demand by 8–10% while maintaining thermal comfort within safe and comfortable ranges.
- To achieve the same level of peak load reduction, jointly adjusting fan speed, rather than solely thermostat setpoint, improves thermal comfort by 5% in the test case.

1. Introduction

Heatwaves are extended periods of high temperature that affect lifestyle and lead to health consequences (Robinson 2001). Under the trend of climate change and global warming, heatwaves will become longer, more frequent, and stronger (Baldwin et al. 2019). It is found that exposure to heatwaves could lead to heat stress (Kovats and Hajat 2008). In quantifying heat stress, degree of thermal discomfort is shown to be a useful measurement (Macpherson 1973). Intensified heat stress would increase health risks (Basu and Samet 2002), such as cardiovascular mortality and respiratory illnesses (Patz et al. 2002) or even cause heat related deaths (Klenk, Becker, and Rapp 2010).

Research has shown for the indoor environment, under heat waves, the presence of air conditioning would significantly reduce the mortality rate (Nunes et al. 2011; Vandentorren et al. 2006). However, as the outdoor temperature rises, the increased energy consumption due to efficiency degradation of the air conditioner and growing demand would increase peak load, which poses great challenges to the grid and could possibly lead to grid shutdown and power outage (Alawadhi and Phelan 2022; Yang, Nishikawa, and Motter 2017). Under heatwaves the peak electric demand (Yau and Hasbi 2013) and the reliability of the grid (Ward 2013) have become particular problems. To respond to the peak load, extending generation, transmission and distribution capacities

---

CONTACT Zhujing Zhang ✉ stellazz@alum.mit.edu ⊙ Department of Architecture, Massachusetts Institute of Technology, 77 Massachusetts Avenue, Cambridge, MA 02139, USA

are conventional approaches, which are costly and practically not efficient considering the small percentage of time peak load occurs in the time span of general usage (Mishra and Palanisamy 2018). The power loss during transmission is in a nonlinear relationship with the current; during the peak load, an increase of the supplied current would result in less efficiency in power transmission (Prasanna 2014).

Studies on building adaptation have developed strategies to mitigate the impacts of heatwaves. In particular, Porritt et al. (2012) rank building-level interventions for reducing overheating under heatwaves. Simson, Kurnitski, and Maivel (2017) identify intervention guidance for building parameters, including orientation, window-to-wall ratios, and overhang dimensions that prevent summer overheating. In addition, authors (Coniff 1991; Braun 2003) show that thermal mass of a building enables reductions in the peak air conditioning load. Given weather variability, the case study in Kneifel and O'Rear (2017) shows that a highly efficient building envelope not only leads to greater peak demand reduction but also improves thermal comfort. Although building adaptations show benefits in mitigating the impacts of heatwaves, the cost and time associated with the construction would be a factor that cannot be neglected.

As an alternative to building renovations, optimizing the operation of air conditioning systems can reduce peak load (Celik et al. 2017; Jeddi, Mishra, and Ledwich 2021). Scheduling, a form of energy management, could reduce renovation costs and efforts, but generally requires some investment in sensing, communication, and controls. Corbin, Henze, and May-Ostendorp (2013) describe a model predictive control method that generates hourly cooling setpoints to minimize the daily energy cost of a commercial building. Price-based energy management can reduce peak load (Xu et al. 2015; Torriti 2012). However, these approaches often underemphasize the thermal comfort of building occupants, a critical metric under heatwaves.

As a complement to air-conditioning, ceiling-mounted or other fans can improve energy efficiency (Yang et al. 2015) by providing more comfortable air movement to occupants (Fountain and Arens 1993; Ho, Rosario, and Rahman 2009; Atthajariyakul and Lertsatittanakorn 2008). The study of Hsiao, Lin, and Lo (2016) optimizes ceiling fan airspeed to enhance thermal comfort and reduce electricity cost. At a group level, a coordinated optimization of a system of fans is able to incorporate the thermal comfort of multiple occupants in one room (Liu et al. 2018).

However, there is limited research on jointly optimizing the control of air conditioners and fans to mitigate both peak load and heat stress. In Luo et al. (2021), Luo et al. evaluate thermal comfort under various constant room temperatures with different fan operating modes and find that a higher setpoint with fan-assisted cooling can achieve similar thermal comfort to a lower setpoint. In Taylor, Brown, and Rim (2021), Taylor et al. run large iterations of EnergyPlus simulations to find optimal air conditioner and fan schedules that reduce total energy usage and ensure thermal comfort. Although the studies of Luo et al. (2021) and Taylor, Brown, and Rim (2021) considered both the air conditioner and fan, Luo et al. (2021) only present analytical results under defined constant settings without means for adjustment, and the optimization strategy by Taylor, Brown, and Rim (2021) is limited by extensive computing required by EnergyPlus simulations. Moreover, in neither of the studies is peak load considered, which is critical under heatwaves.

This paper proposes methods to jointly optimize the air conditioner and fan schedules that mitigate peak load and heat stress under heatwaves. The proposed methods have several practical advantages. They require no building or equipment modelling, which allows flexibility in the application and avoids the need to spend costly expert time on model development. The methods require relatively little data, which protects user privacy. Computationally, the methods efficiently produce optimal schedule adjustments, enabling deployment in real buildings. Recent rapid development and wide use of smart home devices make feedback and control of the cooling systems possible (Lee and Zhang 2021; Yammen, Tang, and Vennapusa 2019). Working with smart devices, the proposed method is able to record, predict and adjust the environmental conditions and power consumption and promote users' thermal satisfaction.

The details of the methods involve (1) learning models to predict baseline demand power and thermal comfort values, (2) training models that relate the adjustments of the fan and air conditioner schedules to the perturbation of demand power and thermal comfort values, and (3) feeding baseline and perturbation models to the optimizer to optimize air conditioner and fan schedules that mitigate the peak load and heat stress. Extending the framework presented by Kircher et al. (2021), for scheduling parameters, the proposed workflows allow adjustments of the fan to be jointly scheduled with the air conditioner and extend the goals to mitigating both peak load and heat stress. A detailed explanation of the method will be shown in Section 1 of this paper.

Although the proposed methods are designed to be implementable in real buildings, to test and demonstrate them, simulation-based implementations are presented in Section 2. Energyplus (2021), a commonly used physics-based building energy simulation tool, is used to obtain data. The Standard Effective Temperature (SET^*) is adopted as a comprehensive measure of thermal

comfort (Gagge, Nishi, and Gonzales 1972; Auliciems and Szokolay 1997). Section 3 describes the workflow tested on a single building and a six-building neighbourhood during a heatwave. Section 4 presents the results. The case studies show that by jointly optimizing air conditioner setpoints and ceiling fan speeds, the methods are able to reduce peak load by 8–10% while maintaining *SET** within comfortable ranges.

2. Methods

The methods proposed in this paper include three phases: baseline model learning (Section 2.1), perturbation model training (Section 2.2), and optimization (Section 2.3). Figure 1 demonstrates the workflow of the proposed methodology.

2.1. Baseline model learning

The goal of this section is to learn surrogate models that predict baseline power load and heat stress conditions in the defined time interval. The building power load records the power usage, a peak in which would result in grid pressure. Load data can be collected from electricity meters. The degree of thermal discomfort is often used as a measurement of heat stress (Macpherson 1973). There are two schools of thermal comfort models, the heat balance model and the adaptive model. Heat balance models consider the human body as a thermodynamic system, which requires the human body to maintain an internal heat balance around $37\pm0.5°$C (Butera 1998). Predictive Mean Vote (*PMV*) (Fanger 1970) and Standard Effective Temperature (*SET**) (Gagge, Nishi, and Gonzales 1972; Auliciems and Szokolay 1997) are representatives of heat balance models. For the adaptive models, the occupant is assumed to be able to adapt to the environment to improve personal thermal comfort. Research has shown that thermal comfort conditions can be quite personal and relate to such parameters such as culture (Brager

and de Dear 2003), age (Indraganti and Rao 2010), and gender (Karjalainen 2007). Building on the knowledge from these thermal comfort models, the recent development of machine learning algorithms and smart sensors has enabled great progress in data-driven models for personalized thermal comfort (Ferreira et al. 2012; Bermejo et al. 2012; Megri, Naqa, and Haghighat 2005; Peng and Hsieh 2017). To mitigate heat stress, it is important to maintain thermal comfort in a comfortable range.

Baseline conditions are set up for the air conditioner and fan, the two devices that this paper is scheduling. Recent fast development and wide application of smart-home devices have opened up the potential for data collection and smart control of household devices. Lee and Zhang (2021) use the data of smart meters and smart thermostats of the air conditioners to predict and control the load in residential buildings; in the paper (Yammen, Tang, and Vennapusa 2019), Yammen et al. offer methods to control the speed of the fan through a mobile application. The baseline schedule of the air conditioner and fan and the building load collected from the smart meters would be used to train the baseline models. In addition, occupancy factors including the information of the type of the day, time of the day, and occupancy schedules are critical to power consumption (Yun et al. 2012). The occupancy data could be collected through sensor or user logs. For the choice of algorithm, there is a great amount of existing research work that predicts load. Review paper (Zhao and Magoulès 2012) compares the performance of various algorithms for load prediction. Artificial Neural Network (ANN) (González and Zamarreño 2005; Ben-Nakhi and Mahmoud 2004) and Support Vector Machine (SVM) (Hou and Lian 2009; Li et al. 2009) are two types of models that can be trained with historical data and obtain high accuracy in prediction however, the models are often complex. The statistical regression model (Hoffman 1998) has more advantages in terms of ease of use, but has less accuracy.
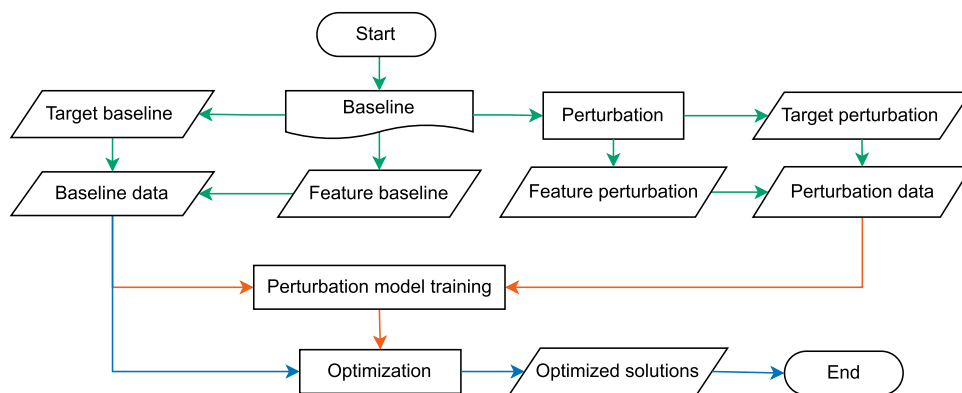

Figure 1. Methodology workflow.

For thermal comfort prediction, the above-mentioned heat balance model, adaptive model, or data-driven personalized thermal comfort model could be used to describe the thermal perception of the occupant. Review paper (Feng et al. 2022) lists input factors for generating thermal comfort values. Normally environmental factors include air temperature, mean radiant temperature, relative humidity, and air speed, which could be measured through a set of sensors (Zhao et al. 2014). Human factors involve anthropometric data, physiological factors, and behavioural factors. The anthropometric data include age, gender, ethnicity, height, and weight, which are often not included in the thermal comfort prediction inputs since the input values would not vary much; the physiological factors often included heart rate, electroencephalogram (EEG), and skin temperature and are the most used inputs for thermal comfort models; the behavioural factors involve lifestyle, clothing insulation, and activity levels, which can be hard to quantify thus often not used in the input data. For the machine learning algorithm, a wide range of models have been applied to predict thermal comfort, including Artificial Neural Network (ANN) (Ferreira et al. 2012; Shan et al. 2020), Fuzzy Logic (Bermejo et al. 2012), and Support Vector Machine (SVM) (Megri, Naqa, and Haghighat 2005; Peng and Hsieh 2017; Alsaleem et al. 2020; Wu, Li, and Qi 2020; Nkurikiyeyezu, Suzuki, and Lopez 2018). Review paper (Feng et al. 2022) points out SVM model is the most used in the reviewed works and obtains one the best prediction accuracies.

The above-mentioned existing machine learning models for power and thermal comfort predictions have their advantages and disadvantages. It would be hard to determine the best model without comparing the performance of a few models for the specific problem with specific requirements for accuracy, computing time, and ease of use. The algorithm of the baseline models could be chosen based on the specific requirements of the problem.

2.2. Perturbation model training

Working with smart meters, smart air conditioner thermostat and fan smart speed control, the perturbation of the air conditioner and fan schedules, power consumption, and thermal comfort are recorded for training the perturbation models. Given the perturbation of the air conditioner and fan schedules, the perturbation models predict the perturbation of load and thermal comfort as output. This paper implements the linear regression proposed by Kircher et al. (2021) as a computationally tractable stand-in for the true system dynamics. Equation (1) is a standard form of linear regression, in which y is the output target vector, X is the input feature matrix, a is the

coefficient vector, and e is the error vector. The coefficient vector a is fit by least squares as shown in Equation (2):

$$y = Xa + e. \tag{1}$$

$$a = (X^TX)^{-1}X^Ty. \tag{2}$$

Consider the power perturbation models with only setpoint perturbation as an example. The perturbation of power is restricted to be linear in the setpoint perturbations:

$$\delta_P(k) = a_1\delta_T(k) + \cdots + a_m\delta_T(k - m + 1) + e_k. \tag{3}$$

In Equation (3), m is a tunable memory parameter, $\delta_P(k)$ and $\delta_T(k)$ are power and temperature perturbations, e_k is the error at time k, and the parameter vector a is fit by least-squares. In the standard linear regression form, $y = Xa + e$, the power perturbation can be written as

$$
\begin{bmatrix} \delta_P(1) \\ \vdots \\ \delta_P(m) \\ \vdots \\ \delta_P(k) \end{bmatrix} = \begin{bmatrix} \delta_T(1) & & \\ \vdots & \ddots & \\ \delta_T(m) & \cdots & \delta_T(1) \\ \vdots & & \vdots \\ \delta_T(k) & \cdots & \delta_T(k-m+1) \end{bmatrix} \begin{bmatrix} a_1 \\ \vdots \\ a_m \end{bmatrix}
$$

$$
+ \begin{bmatrix} e_1 \\ \vdots \\ e_m \\ \vdots \\ e_k \end{bmatrix}. \tag{4}
$$

The coefficient vector a can be identified by least squares estimation: $a = (X^TX)^{-1}X^Ty$. Implementing this paper's proposed method, two perturbation models are trained in Equations (5) and (6), where perturbation of power $\delta_P(k)$ and perturbation of thermal comfort $\delta_C(k)$ are restricted to be linear in the setpoint perturbation $\delta_T(k)$ and fan operation perturbations $\delta_{Fan}(k)$.

$$
\begin{bmatrix} \delta_P(1) \\ \vdots \\ \delta_P(m) \\ \vdots \\ \delta_P(k) \end{bmatrix} = \begin{bmatrix} \delta_T(1) & & & \delta_{Fan}(1) \\ \vdots & \ddots & & \vdots \\ \delta_T(m) & \cdots & \delta_T(1) & \delta_{Fan}(m) \\ \vdots & \ddots & \vdots & \vdots \\ \delta_T(k) & \cdots & \delta_T(k-m+1) & \delta_{Fan}(k) \end{bmatrix}
$$

$$
\begin{bmatrix} \ddots & & \\ \cdots & \delta_{Fan}(1) & \\ \ddots & \vdots & \\ \cdots & \delta_{Fan}(k-m+1) \end{bmatrix} \begin{bmatrix} a_1 \\ \vdots \\ a_m \\ a_{m+1} \\ \vdots \\ a_{2m} \end{bmatrix} + \begin{bmatrix} e_{1_P} \\ \vdots \\ e_{m_P} \\ \vdots \\ e_{k_P} \end{bmatrix}
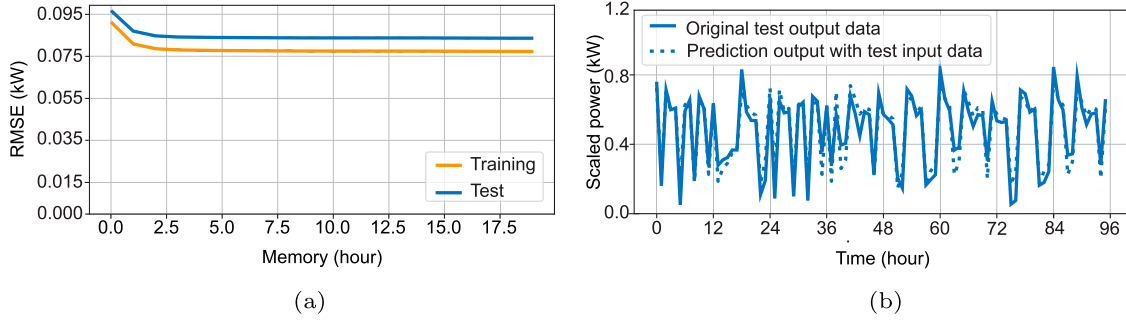$$

$$\tag{5}$$

Figure 2. Surrogate model training. (a) Surrogate model training RMSE convergence and (b) Test data and prediction comparison.

$$
\begin{bmatrix} \delta_C(1) \\ \vdots \\ \delta_C(m) \\ \vdots \\ \delta_C(k) \end{bmatrix} = \begin{bmatrix} \delta_T(1) & & & \delta_{Fan}(1) \\ \vdots & \ddots & & \vdots \\ \delta_T(m) & \dots & \delta_T(1) & \delta_{Fan}(m) \\ \vdots & \ddots & \vdots & \vdots \\ \delta_T(k) & \dots & \delta_T(k-m+1) & \delta_{Fan}(k) \end{bmatrix}
$$

$$
\begin{matrix} \ddots & & \\ \dots & \delta_{Fan}(1) & \\ \ddots & \vdots & \\ \dots & \delta_{Fan}(k-m+1) \end{matrix} \begin{bmatrix} b_1 \\ \vdots \\ b_m \\ b_{m+1} \\ \vdots \\ b_{2m} \end{bmatrix} + \begin{bmatrix} e_{1_{SET}} \\ \vdots \\ e_{m_{SET}} \\ \vdots \\ e_{k_{SET}} \end{bmatrix}
$$

$$(6)$$

With the case study data in Section 4.1, the power perturbation model's Root Mean Square Error (*RMSE*) convergence over the manually tuned memory number m is shown in Figure 2(a). Figure 2(b) shows a comparison of the power prediction from the trained perturbation model (in dotted line) with the power consumption data from the test data (in solid line) over 96 hours.

2.3. CVX optimization

In the third step, the trained baseline and perturbation models are fed into the load-shifting optimization. The goal of the optimization is to determine air conditioner and fan schedule perturbations that minimize the weighted sum of the peak power and thermal comfort value over a day. The objective goal can be written as a weighted sum,

$$
P_{\text{weight}} \cdot \max(P_{\text{base}} + \delta_P) + C_{\text{weight}} \cdot \max(C_{\text{base}} + \delta_C),
$$
$$(7)$$

where P_{weight} and C_{weight} are assigned weights leading to an optimized reduction of peak power and the magnitude of a thermal comfort index above a discomfort threshold. Since the proposed methods use a linear regression model as the surrogate, a convex solver, CVXpy (Diamond and Boyd 2016), can be applied to solve

the optimization problems. The surrogate and optimizer choices in the proposed methods guarantee that the optimization problems can be solved to global optimality. Furthermore, the workflow results in very low computation costs in solving such multi-objective optimization problems with high dimensional variables in hourly or even smaller increments. The computational efficiency makes the proposed methods better suited for implementation in home-automation systems.

3. Simulation-based implementation

Although proposed methods are intended to be implementable in real buildings, we demonstrate them through simulation. This implementation uses the Standard Effective Temperature (*SET**), one of the comprehensive measures of thermal comfort that describes the 'feels like' temperature (Gagge, Nishi, and Gonzales 1972; Auliciems and Szokolay 1997), as the measurement of thermal comfort. Data are obtained from simulation with a commonly used physics-based building energy simulation tool, Energyplus (2021), which is able to capture the efficiency change of air conditioning systems under heatwaves.

For baseline conditions, this study uses the single-family prototype model in the ASHRAE 1A climate zone (very hot-humid) published by the Building energy codes program (2021). The Miami TMY3 epw file is used as a weather file for the simulation. Figure 3(a) shows the outdoor temperature over a year of the chosen climate profile. The summer hottest day, shown in Figure 3(b), is set as the optimization day. Researchers at the Pacific Northwest National Laboratory developed the prototype model as a standard test-case for single-family homes. The prototype is a two-story house with a floor area of $110 \, \text{m}^2$ for each floor, and window-wall ratio of 0.15 on each side of the building. The wall R value is $1.9 \, \text{m}^2\text{K/W}$ and window U value is $2.8 \, \text{W/m}^2\text{K}$. The two stories are set as one conditioned zone, and the attic is set as an unconditioned zone. Power consumption and thermal performance are monitored in the conditioned zone for
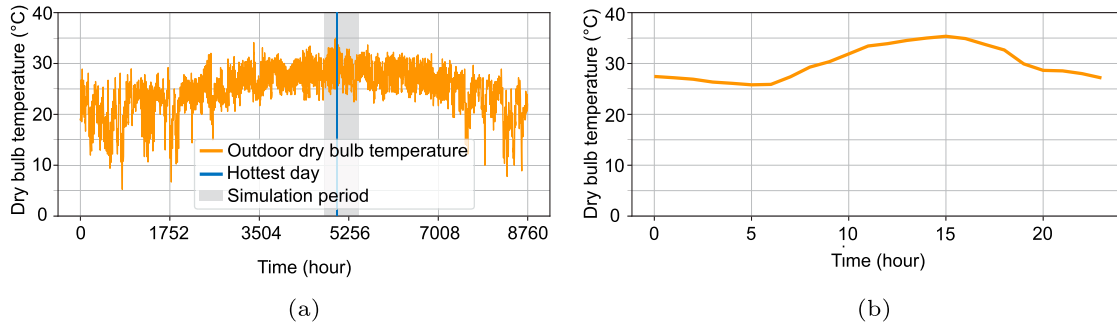
Figure 3. Outdoor dry bulb temperature in one year and the hottest day. (a) Outdoor dry bulb temperature (whole year) and (b) Outdoor dry bulb temperature (hottest day).
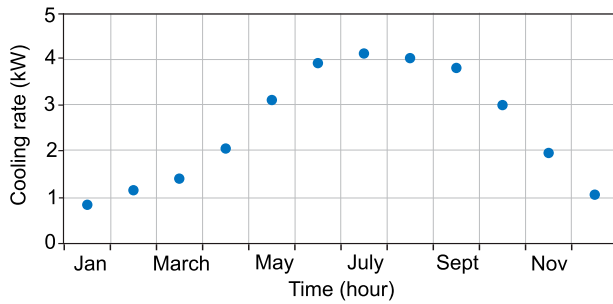

Figure 4. Cooling coil total cooling rate.

the case study. The annual total energy use of the facility is 16,086 kWh, with 6476 kWh of HVAC power consumption. The air conditioner in the prototype is a Unitary Heat Pump Air to Air system with a direct expansion coil for cooling which has the designed gross rated cooling capacity of 6.79 kW. The cooling coil's monthly average cooling rate over the year is shown in Figure 4.

The baseline setpoint keeps the default value at $\hat{T}(k) = 23.9°C$. In addition to the air conditioning system, raising air speed by fans is an energy-efficient strategy (Yang et al. 2015) that could benefit thermal comfort (Atthajariyakul and Lertsatittanakorn 2008; Ho, Rosario, and Rahman 2009). The values of average air speed and power consumption of the ceiling fan refer to the data published by Liu et al. (2018). A baseline air speed of 0.35 m/s is implemented in this test with an average power consumption of 0.48 W/m². An hourly baseline power $\hat{P}(k)$ and Standard Effective Temperature $\hat{SET}(k)$ are generated as the baseline target. Since EP simulations are able to generate $\hat{P}(k)$ and $\hat{SET}(k)$, the step of baseline model learning is skipped in this study. Under the heatwave context in this paper, the hottest day and four weeks around the hottest day are simulated.

eppy (2021) is used to parametrically modify the schedules of the cooling systems. The perturbation range for setpoint is $\pm 3°C$ and for air speed is ± 0.35 m/s. The ranges of perturbation are set that would not cause dramatic changes to the thermal conditions but are enough to create useful signals to train the perturbation model. For the target perturbation, at time k, the perturbation of power is calculated as $P(k) - \hat{P}(k)$; the perturbation of SET^* is calculated as $SET(k) - \hat{SET}(k)$. A pseudo-random binary sequence (PRBS) of setpoint and air speed in the defined ranges is used to simulate the perturbation of power and SET^*. Linear regression models as explained in Section 2.1 are implemented and trained as a surrogate for EP using the perturbation data of setpoint and air speed as input and the perturbation of power and SET^* as output. One model for power perturbation and one model for SET^* perturbation are trained to relate changes of setpoint and air speed to the changes of power and SET^*.

Given the baseline data and trained surrogate model, the optimization to determine setpoint and air speed perturbations that minimize the weighted sum of the peak power and SET^* over a day is implemented with the process demonstrated in Section 2.2.

4. Case study

This section demonstrates the proposed methodology with a single building case study and a six-building neighbourhood case study. The details of the baseline model and weather condition for the case studies are provided in Section 2. The baseline air conditioner and fan setting can be found in the same section.

With the constant default setpoint at 23.9°C and air speed at 0.35 m/s, the baseline hourly power consumption and SET^* are shown in Figure 5(a,b). The power demand and SET^* in the optimization day are used as a baseline for the case study. Figure 5(a) shows, that as the outdoor temperature rises in the afternoon, the baseline power demand in the afternoon increases and reaches a peak, due to the increased thermal load and the decreased cooling system efficiency when the
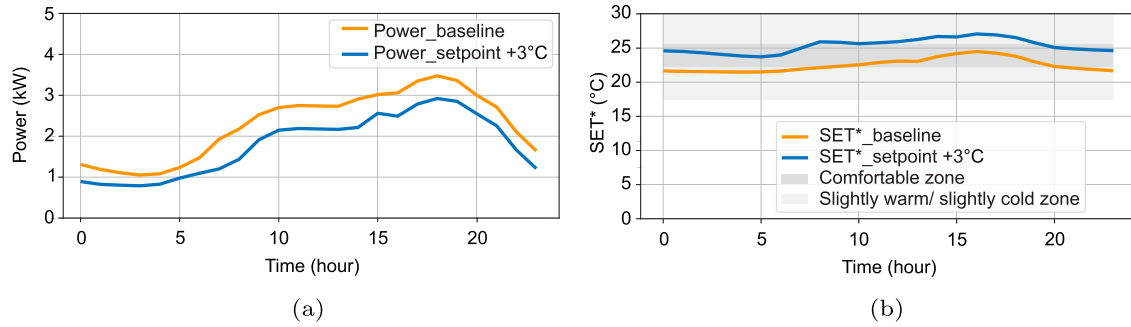
Figure 5. Power and *SET** in the hottest day. (a) Hottest day power consumption and (b) Hottest day *SET**.

temperature difference between outdoor and indoor increases. To reduce the peak power, one easy solution would be raising the constant setpoint. If the setpoint is raised 3°C, the resulting hourly power consumption is shown in the same figure. Although the easy approach shifts the curve of power consumption down, it compromises *SET** as shown in Figure 5(b). The darker grey and lighter grey shading boxes in Figure 5(b) indicate the thermally comfortable zone (22.2–25.6°C) and the lightly warm/cold zone (17.5–22.2°C, 25.6–30°C) of *SET** (Auliciems and Szokolay 1997). The goal for the optimization of the case studies below is to reduce the peak load and maintain a thermally comfortable condition.

4.1. Single building

The single building case study model shown in Figure 6(a) uses the single-family residential prototype model of the 1A climate zone demonstrated in Section 2 as a baseline.

The hourly baseline power $\hat{P}(k)$ and Standard Effective Temperature $S\hat{E}T(k)$ of the prototype model are generated as baseline targets. The hottest day and four weeks around the hottest day are set as the run period. To generate perturbation data, eppy (2021) is used to parametrically modify the schedules of the setpoint and air speed. The perturbation ranges for setpoint and air speed are demonstrated in Section 2. One hundred fifty sets of schedule perturbations are generated.

One perturbation model for power and one perturbation model for *SET** are trained with linear regression functions in Equations (5) and (6). The baseline power and *SET** and the trained power and *SET** perturbation models are fed into the convex linear solver, CVXpy (Diamond and Boyd 2016) with goal function in Equation (7). The proposed methods require low computation cost in solving the high-dimensional multi-objective optimization problems. A multi-objective sampling is applied with 1000 different combinations of randomly generated P_{weight} and S_{weight} assigned to the optimization function (7). For the demonstration purpose of the case study, an optimized solution of 75% P_{weight} to peak power reduction, and 25% S_{weight} to peak *SET** reduction is shown in the result Section 5.1.

As shown in Figures 8(a,b) and 9(a,b), comparing the surrogate predictions outputted from the optimizer and the *EP* simulation outputs with the optimizer generated schedules, the relative error is within 8%. Although the relative error is quite small, since it is a surrogate prediction, there would still be some error compared to a physics-based simulation.

4.2. Six-building neighbourhood

The six-building neighbourhood, as shown in Figure 6(b), is composed of six single-family buildings with various footprints derived from the prototype single-family
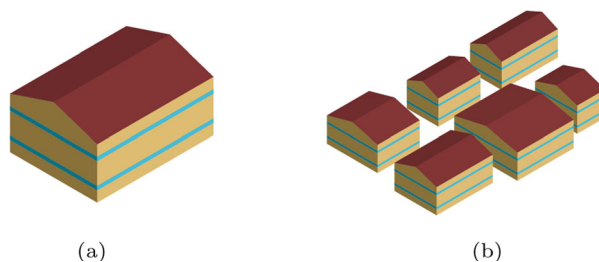

Figure 6. Case study models. (a) Single building model and (b) Six-building neighbourhood model.

model. A python package, geomeppy (2021), which facilitates geometric changes of the EP model including dimension, orientation and window wall ratio, is used to make the geometry modification of the prototype model. The footprint of the buildings on each floor varies from 55 to 165 m^2. The window wall ratio of the buildings remains at 0.15 on each side of the buildings.

The process of baseline and perturbation data generation and perturbation model training is repeated for each of the six units. as described in Section 4.1. For each unit, one perturbation model for power and one perturbation model for SET^* are trained with their respective linear regression function (5) (6). The baseline power and SET^* and the trained power and SET^* perturbation models of the six units are fed into the convex linear solver, CVXpy (Diamond and Boyd 2016). The goal of the optimization for the six-unit neighbourhood case study is
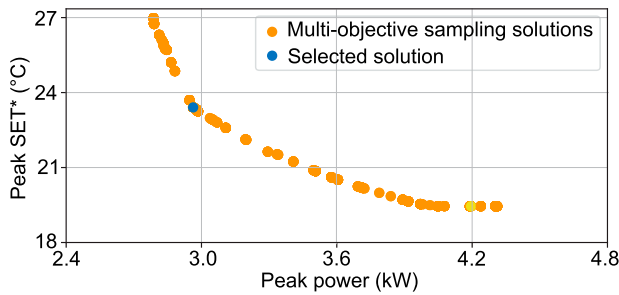
to reduce the aggregate peak power and SET^* of the six units. Similarly, a multi-objective sampling is applied with 1000 different combinations of randomly generated P_{weight} and S_{weight} assigned to the optimization goal. To show a set of results in different weights, Section 5.2 presents the optimized solution of assigning 65% P_{weight} to peak power reduction, and 35% S_{weight} to peak SET^* reduction.

5. Results

5.1. Single building

As shown in Figure 7, the multi-objective sampling method gives a range of optimized solutions to the case-study problem. The solutions form a Pareto Front (Legriel et al. 2010), in which each dot in the figure represents one unique optimal solution that cannot improve in one dimension without compromising the other. The highlighted dot in Figure 7 demonstrates the optimal solution of 75% P_{weight} to peak power optimization and 25% S_{weight} to peak SET^* optimization for the single building case study. Figure 8(a,b), shows the baseline performance, the surrogate prediction from the optimizer, and the building performance from EP simulation with the optimizer-generated schedules. As indicated in both figures, the optimized peak power and SET^* are reduced by 8% and 3% compared to the baseline. To reduce peak load, the optimized schedules provide additional cooling prior to the peak period; some of the energy is

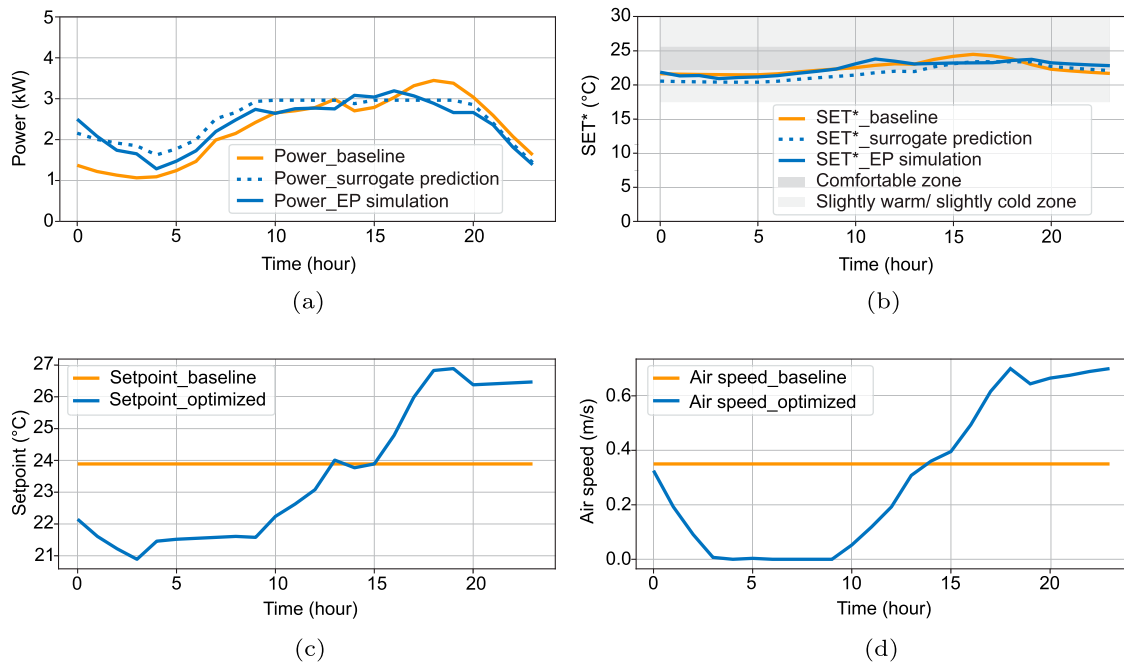**Figure 7.** Single-building multi-objective sampling.

Figure 8. Single-building optimized solution. (a) Single-building power; (b) Single-building SET^*; (c) Single-building setpoint schedule and (d) Single-building air speed schedule.

lost due to increased conduction through the building envelope associated with a large indoor-outdoor temperature difference, which results in the increase of total energy consumption by 5%. The schedules of cooling system setpoint and ceiling fan air speed that result in the reduction are shown in Figure 8(c,d). The optimized setpoint solution pre-cools the building earlier in the morning then raises the setpoint temperature in the afternoon when the outdoor temperature increases. To maintain the indoor environment at a thermally comfortable level, the ceiling fan schedule raises the air speed in the afternoon.

Table 1. Single-building peak power and *SET** under different scheduling methods.

	$P_{difference}$%	$SET_{difference}$%
Setpoint scheduling	−8 %	+2 %
Setpoint + Air speed scheduling	−8 %	−3 %

A comparison study of only adjusting the setpoints of the air conditioner is done. As shown in Table 1, to achieve 8% peak load reduction if adjusting only cooling setpoints, the peak *SET** will increase by 2%. The comparison shows the advantage of jointly adjusting both setpoints and air speed for peak load and heat stress mitigation.

5.2. Six-building neighbourhood

For the six-building neighbourhood, with 65% P_{weight} assigned to peak power optimization and 35% S_{weight} assigned to peak *SET** optimization, Figure 9(e,f) shows the methodology is able to provide coordinated setpoint and air speed schedules for the small community. Figure 9(c,d) present the coordinated individual power and *SET** of the six buildings. As shown in Figure 9(a,b), the aggregate peak power is reduced 10% compared to the baseline and the average *SET** increases by only 2%.
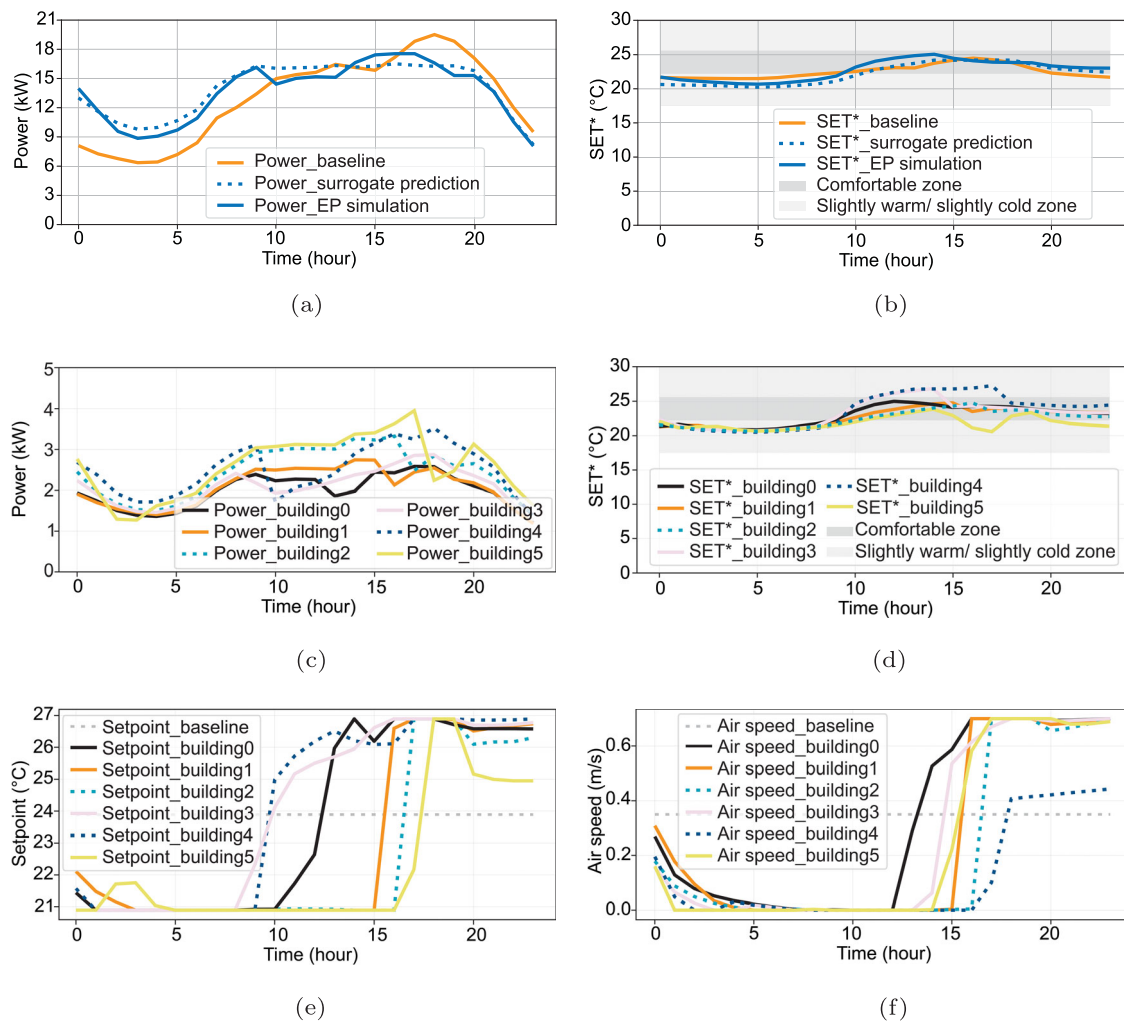

Figure 9. Six-building jointly optimized solutions. (a) Six-building aggregated power; (b) Six-building average *SET**; (c) Six-building individual power; (d) Six-building individual *SET**; (e) Six-building setpoint schedules and (f) Six-building air speed schedules.
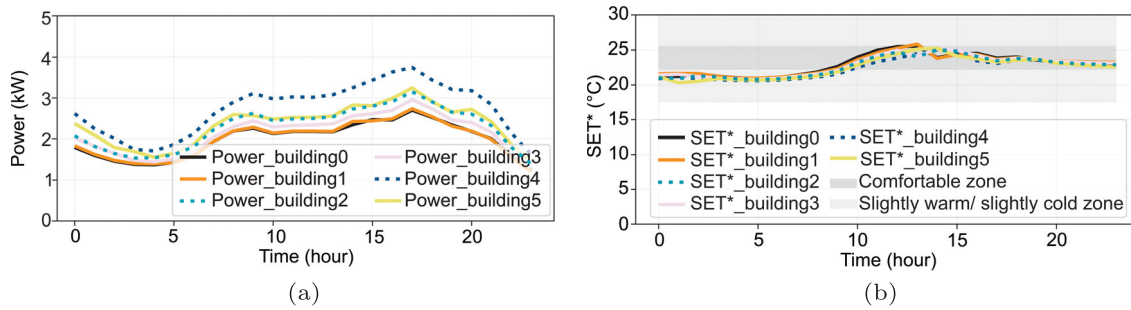
Figure 10. Six-building individually optimized solutions. (a) Six-building individual power and (b) Six-building individual *SET**.

Over the whole day the total energy of the optimized solution increases 6%.

To compare with the neighbourhood-level joint optimization, a test was done by optimizing the schedules of the six buildings individually with the same assigned weights to the same optimization goal. Figure 10(b) shows the result SET of the individual building, which are all within the comfortable range. For the optimized power, as shown in Figure 10(a), the individually optimized power profiles all peak at the same time, which will result a new accumulated peak load. Comparing with the baseline, the new aggregate peak of the individually optimized solutions reduced only 5%, which is 5% less than the jointly optimized solutions. Although jointly optimizing the scheduling in a neighbourhood level would required sharing and communicating certain data, the

coordinated optimization is able to reduce the peak load further.

5.3. Single-building wall R value and window U value variations

In addition to the schedule optimization, building-level interventions such as wall R value and window U value influence the power consumption. Building off the single unit case study, this section demonstrates the result of the single-building optimization with wall R value varying from 1.9 to 3.4 m^2K/W, and window U value varying from 1.1 to 4.5 W/m^2K. The proposed methodology is applied to the single buildings with wall R value of 1.9, 2.2, 2.5, 2.8, 3.1, 3.4 m^2K/W. Similarly, the process is repeated for each of the buildings with window U value of 1.1, 2.8,
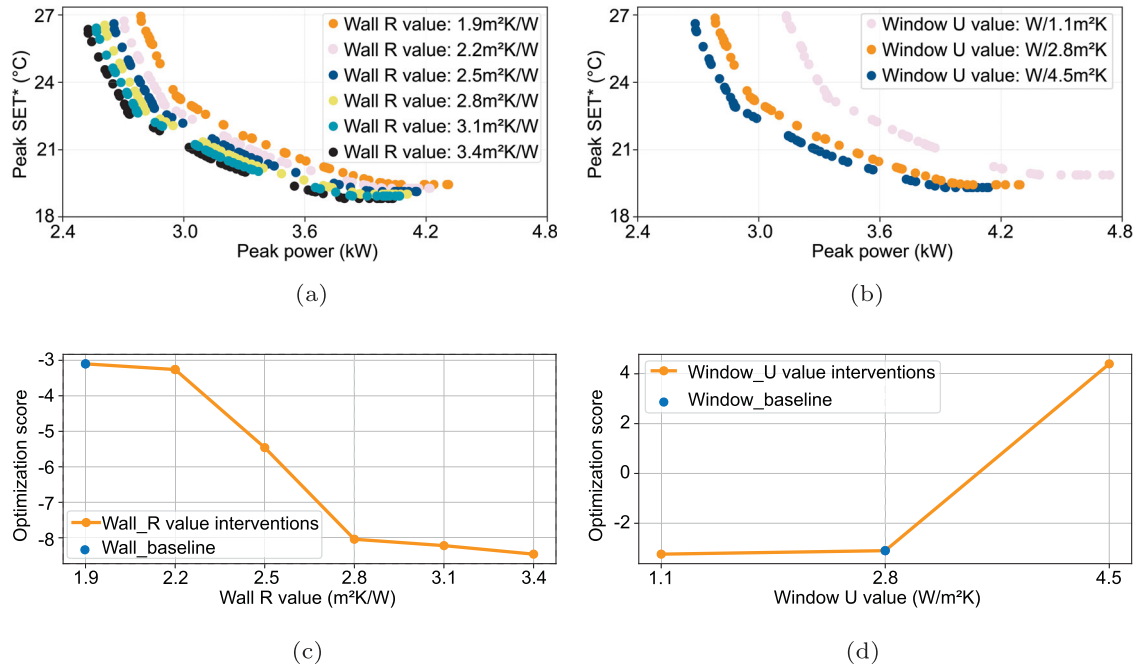

Figure 11. Multi-objective sampling (moo) and optimization score ($score_{opt}$) with wall R value from 1.9 to 3.4 m^2K/W and window U value from 1.1 to 4.5 W/m^2K. (a) Moo with wall R value variations; (b) Moo with window U value variations; (c) $Score_{opt}$ with wall R-value variations and (d) $Score_{opt}$ with window U value variations.

and 4.5 W/m^{2}K. Figure 11(a,b) present a wide range of solutions from the multi-objective sampling with wall R value and window U value variations. In both plots, the X-axis represents the optimized peak power and Y-axis represents the optimized peak SET^*.

Figure 11(a,b) show that as the wall R value increases and the window U value decreases, the Pareto Front moves closer to the origin. The baseline peak power and SET^* of the prototype model with default wall R value of 1.9 m^{2}K/W and window U value of 2.8 W/m^{2}K are used for comparison. To cross-compare the results of the optimization, an optimization score is introduced here:

$$\text{score}_{opt} = P_{\text{weight}} \cdot P_{\text{change}}\% + SET_{\text{weight}} \cdot SET_{\text{change}}\%$$

(8)

In Equation (8), P_{weight} and S_{weight} are the weights assigned to peak power and peak SET^* optimization. The value of P_{weight} and S_{weight} are 60% and 40% in this result section. P_{change} and SET_{change} are peak power and SET^* changes compared to the baseline peak power and SET^* of the prototype model. Smaller optimization scores indicate better optimization results. The optimization score with wall R value and window U value variation are shown in Figure 11(c,d). Figure 11(c) shows that as wall R value changes from 1.9 to 2.8 m^{2}K/W, there is a significant improvement in the optimization score; after 2.8 m^{2}K/W, although the optimization score still improves as the R value increases, the magnitude of improvement is smaller. For the window U value variation, Figure 11(d) shows the decrease of the optimization score is sharper as the window U value changes from 4.5 to 2.8 W/m^{2}K than from 2.8 to 1.1 W/m^{2}K.

6. Conclusion and discussion

This paper proposes methods to adjust air conditioner and fan schedules that mitigate demand peak and heat stress under heatwaves. The results show that by jointly optimizing the control of the air conditioner and fan, the methods are able to identify with low computing cost cooling equipment schedules that mitigate the peak power and heat stress under the heat event.

At the neighbourhood level, jointly optimizing the scheduling among the households shows more advantage in peak load reduction than separately scheduling individual households. For building-level interventions such as wall R value and window U value, the results show that as the wall R-value increases and the window U value decreases, the scheduling methods in general are able to generate better solutions for peak load and heat stress mitigation. As a next step, the proposed methods have great potential to integrate with other heat resilient strategies such as improvements in insulation, solar shading, and thermal mass.

The methods are implementable in real buildings with no need for building energy models. The perturbation of the building system would generate data needed to train the perturbation models. Although field demonstration is not part of this work, a similar methodology was recently implemented in an experiment in a university classroom to reduce total energy use and carbon emissions (Cai 2022).

The trained baseline and linear regression perturbation models are able to generate close predictions of the load and thermal comfort conditions. The choice of the surrogate models and optimizer ensures computing speed and global optimality of the solutions. Increased prediction accuracy can be achieved by adopting a non-linear perturbation model, however, the optimization would require more time to converge and may give solutions that are local minima.

The perturbation models demonstrated in this paper are based on defined perturbation ranges. For changes in these conditions, new perturbation models would need to be trained with new data of load and thermal comfort value perturbation. To offer large-scale solutions, a separate surrogate model that is able to predict the perturbation values for various perturbation ranges would be necessary.

The implementation of the proposed method is able to be achieved in real buildings by inputting optimized schedules to air conditioner smart thermostats and fan smart speed controls such as the devices mentioned in papers (Özgür et al. 2018; Yammen, Tang, and Vennapusa 2019). Although the hardware of these devices has been rapidly developed, the control complexity is still limited (Lee and Zhang 2021). As the evolving capability of smart devices allows more complex control algorithms to be implemented, they would be able to archive more customized goals such as reducing peak load and ensuring thermal comfort at meantime.

This paper demonstrates the methods with thermostat setpoint and fan speed schedule optimization; the framework could extend the optimization features to other building operational schedules. In addition to the optimization target demonstrated here – peak load and heat stress mitigation – the methodology could be applied to an extended range of goals such as total energy usage, carbon emissions, and electricity costs.

Acknowledgments

References

Alawadhi, M., and P. E. Phelan. 2022. "Review of Residential Air Conditioning Systems Operating under High Ambient Temperatures." *Energies* 15 (8): 2880. doi:10.3390/en15082880.

Alsaleem, F., M. K. Tesfay, M. Rafaie, K. Sinkar, D. Besarla, and P. Arunasalam. 2020. "An Iot Framework for Modeling and Controlling Thermal Comfort in Buildings." *Frontiers in Built Environment* 6 (87): doi:10.3389/fbuil.2020.00087.

Atthajariyakul, S., and C. Lertsatittanakorn. 2008. "Small Fan Assisted Air Conditioner for Thermal Comfort and Energy Saving in Thailand." *Energy Conversion and Management* 49 (10): 2499–2504. doi:10.1016/j.enconman.2008.05.028.

Auliciems, A., and S. V. Szokolay. 1997. "Thermal Comfort." PLEA notes, PLEA in Association with Dept. of Architecture, University of Queensland.

Baldwin, J. W., J. B. Dessy, G. A. Vecchi, and M. Oppenheimer. 2019. "Temporally Compound Heat Wave Events and Global Warming: An Emerging Hazard." *Earth's Future* 7 (4): 411–427. doi:10.1029/2018EF000989.

Basu, R., and J. M. Samet. 2002. "Relation Between Elevated Ambient Temperature and Mortality: A Review of the Epidemiologic Evidence." *Epidemiologic Reviews* 24 (2): 190–202. doi:10.1093/epirev/mxf007.

Ben-Nakhi, A. E., and M. A. Mahmoud. 2004. "Cooling Load Prediction for Buildings Using General Regression Neural Networks." *Energy Conversion and Management* 45 (13–14): 2127–2141. doi:10.1016/j.enconman.2003.10.009.

Bermejo, P., L. Redondo, L. de la Ossa, D. Rodríguez, J. Flores, C. Urea, J. A. Gámez, and J. M. Puerta. 2012. "Design and Simulation of a Thermal Comfort Adaptive System Based on Fuzzy Logic and on-line Learning." *Energy and Buildings* 49: 367–379. doi:10.1016/j.enbuild.2012.02.032.

Brager, G. S., and R. J. de Dear. 2003. "Historical and Cultural Influences on Comfort Expectations." In *Buildings, Culture and Environment: Informing Local and Global Practices*, 177–201. John Wiley & Sons, Ltd. https://onlinelibrary.wiley.com/doi/abs/10.1002/9780470759066.ch11. doi:10.1002/9780470759066.ch11.

Braun, J. E. 2003. "Load Control Using Building Thermal Mass." *Journal of Solar Energy Engineering* 125 (3): 292–301. doi:10.1115/1.1592184.

Building energy codes program. 2021. "Prototype Building Models." Accessed November 17, 2021. https://www.energycodes.gov/prototype-building-models.

Butera, F. M. 1998. "Chapter 3–principles of Thermal Comfort." *Renewable and Sustainable Energy Reviews* 2 (1–2): 39–66. doi:10.1016/S1364-0321(98)00011-2.

Cai, Y. 2022. "Simulation-and Experiment-Based Setpoint Control for Heating, Ventilation, and Air-Conditioning Systems: A Single- and Multi-Objective Optimization Problem." Master Thesis, Massachusetts Institute of Technology.

Celik, B., R. Roche, D. Bouquain, and A. Miraoui. 2017. "Coordinated Neighborhood Energy Sharing Using Game Theory and Multi-Agent Systems." In *2017 IEEE Manchester PowerTech*, 1–6. IEEE. doi:10.1109/PTC.2017.7980820.

Coniff, J. 1991. "Strategies for Reducing Peak Air Conditioning Loads by Using Heat Storage in the Building Structure." *ASHRAE Transactions* 97 (1): 704–709.

Corbin, C. D., G. P. Henze, and P. May-Ostendorp. 2013. "A Model Predictive Control Optimization Environment for Real-Time Commercial Building Application." *Journal of Building Performance Simulation* 6 (3): 159–174. doi:10.1080/19401493.2011.648343.

Diamond, S., and S. Boyd. 2016. "CVXPY: A Python-Embedded Modeling Language for Convex Optimization." *Journal of Machine Learning Research* 17 (83): 1–5.

Energyplus. 2021. Accessed November 17, 2021. https://energyplus.net/.

eppy. 2021. Accessed November 17, 2021. https://github.com/santoshphilip/eppy.

Fanger, P. O. 1970. "Thermal Comfort. Analysis and Applications in Environmental Engineering." In *Thermal Comfort. Analysis and Applications in Environmental Engineering*.

Feng, Y., S. Liu, J. Wang, J. Yang, Y.-L. Jao, and N. Wang. 2022. "Data-Driven Personal Thermal Comfort Prediction: A Literature Review." *Renewable and Sustainable Energy Reviews* 161: 112357. doi:10.1016/j.rser.2022.112357.

Ferreira, P., A. Ruano, S. Silva, and E. Conceição. 2012. "Neural Networks Based Predictive Control for Thermal Comfort and Energy Savings in Public Buildings." *Energy and Buildings* 55: 238–251. doi:10.1016/j.enbuild.2012.08.002.

Fountain, M., and E. Arens. 1993. "Air Movement and Thermal Comfort." *Ashrae Journal – ASHRAE J* 35: 26–29.

Gagge, A., J. Nishi, and R. Gonzales. 1972. "Standard Effective Temperature - A Single Temperature Index of Temperature Sensation and Thermal Discomfort." Proceeding of the CIB commission W45 symposium: 229–50.

geomeppy. 2021. Accessed November 17, 2021. https://github.com/jamiebull1/geomeppy.

González, P. A., and J. M. Zamarreño. 2005. "Prediction of Hourly Energy Consumption in Buildings Based on a Feedback Artificial Neural Network." *Energy and Buildings* 37 (6): 595–601. doi:10.1016/j.enbuild.2004.09.006.

Ho, S. H., L. Rosario, and M. M. Rahman. 2009. "Thermal Comfort Enhancement by Using a Ceiling Fan." *Applied Thermal Engineering* 29 (8–9): 1648–1656. doi:10.1016/j.applthermaleng.2008.07.015.

Hoffman, A. 1998. "Peak Demand Control in Commercial Buildings with Target Peak Adjustment Based on Load Forecasting." In *Proceedings of the 1998 IEEE International Conference on Control Applications* (Cat. No.98CH36104), Vol. 2, 1292–1296. IEEE. doi:10.1109/CCA.1998.721669.

Hou, Z., and Z. Lian. 2009. "An Application Of Support Vector Machines In Cooling Load Prediction." In *2009 International Workshop on Intelligent Systems and Applications*, 1–4. IEEE. doi:10.1109/IWISA.2009.5072707.

Hsiao, S.-W., H.-H. Lin, and C.-H. Lo. 2016. "A Study of Thermal Comfort Enhancement by the Optimization of Airflow Induced by a Ceiling Fan." *Journal of Interdisciplinary Mathematics* 19 (4): 859–891. doi:10.1080/09720502.2016.1225935.

Indraganti, M., and K. Rao. 2010. "Effect of Age, Gender, Economic Group and Tenure on Thermal Comfort: A Field Study in Residential Buildings in Hot and Dry Climate with Seasonal Variations." *Energy and Buildings* 42 (3): 273–281. doi:10.1016/j.enbuild.2009.09.003.

Jeddi, B., Y. Mishra, and G. Ledwich. 2021. "Distributed Load Scheduling in Residential Neighborhoods for Coordinated Operation of Multiple Home Energy Management Systems." *Applied Energy* 300: 117353. doi:10.1016/j.apenergy.2021.117353.

Karjalainen, S. 2007. "Gender Differences in Thermal Comfort and Use of Thermostats in Everyday Thermal Environments." *Building and Environment* 42 (4): 1594–1603. doi:10.1016/j.buildenv.2006.01.009.

Kircher, K. J., Y. Cai, L. K. Norford, and S. B. Leeb. 2021. "Controlling Big, Diverse, Nonlinear Load Aggregations for Grid Services By Adjusting Device Setpoints." In *IEEE Conference on Decision and Control*, 8. IEEE.

Klenk, J., C. Becker, and K. Rapp. 2010. "Heat-Related Mortality in Residents of Nursing Homes." *Age and Ageing* 39 (2): 245–252. doi:10.1093/ageing/afp248.

Kneifel, J., and E. O'Rear. 2017. "Reducing the Impacts of Weather Variability on Long-Term Building Energy Performance by Adopting Energy-Efficient Measures and Systems: A Case Study." *Journal of Building Performance Simulation* 10 (1): 58–71. doi:10.1080/19401493.2016.1256431.

Kovats, R. S., and S. Hajat. 2008. "Heat Stress and Public Health: A Critical Review." *Annual Review of Public Health* 29 (1): 41–55. doi:10.1146/annurev.publhealth.29.020907.090843.

Lee, Z. E., and K. M. Zhang. 2021. "Scalable Identification and Control of Residential Heat Pumps: A Minimal Hardware Approach." *Applied Energy* 286: 116544. doi:10.1016/j.apenergy.2021.116544.

Legriel, J., C. Le Guernic, S. Cotton, and O. Maler. 2010. "Approximating the Pareto Front of Multi-Criteria Optimization Problems." In *Tools and Algorithms for the Construction and Analysis of Systems*, edited by J. Esparza, R. Majumdar, 69–83. Lecture Notes in Computer Science, Springer. doi:10.1007/978-3-642-12002-2_6.

Li, Q., Q. Meng, J. Cai, H. Yoshino, and A. Mochida. 2009. "Applying Support Vector Machine to Predict Hourly Cooling Load in the Building." *Applied Energy* 86 (10): 2249–2256. doi:10.1016/j.apenergy.2008.11.035.

Liu, S., A. Lipczynska, S. Schiavon, and E. Arens. 2018. "Detailed Experimental Investigation of Air Speed Field Induced by Ceiling Fans." *Building and Environment* 142: 342–360. doi:10.1016/j.buildenv.2018.06.037.

Liu, S., L. Yin, S. Schiavon, W. K. Ho, and K. V. Ling. 2018. "Coordinate Control of Air Movement for Optimal Thermal Comfort." *Science and Technology for the Built Environment* 24 (8): 886–896. doi:10.1080/23744731.2018.1452508.

Luo, M., H. Zhang, Z. Wang, E. Arens, C. Wenhua, F. Bauman, and P. Raftery. 2021. "Ceiling-Fan-Integrated Air-Conditioning: Thermal Comfort Evaluations." *Buildings and Cities* 2 (1): 928–951. doi:10.5334/bc.137.

Macpherson, R. K. 1973. "Thermal Stress and Thermal Comfort." *Ergonomics* 16 (5): 611–622. doi:10.1080/00140137308924552.

Megri, A., I. E. Naqa, and F. Haghighat. 2005. "A Learning Machine Approach for Predicting Thermal Comfort Indices." *International Journal of Ventilation* 3 (4): 363–376. doi:10.1080/14733315.2005.11683930.

Mishra, S., and P. Palanisamy. 2018. "Efficient Power Flow Management and Peak Shaving in a Microgrid-PV System." In *2018 IEEE Energy Conversion Congress and Exposition (ECCE)*, 3792–3798. IEEE. doi:10.1109/ECCE.2018.8558312.

Nkurikiyeyezu, K. N., Y. Suzuki, and G. F. Lopez. 2018. "Heart Rate Variability as a Predictive Biomarker of Thermal Comfort." *Journal of Ambient Intelligence and Humanized Computing* 9 (5): 1465–1477. doi:10.1007/s12652-017-0567-4.

Nunes, B., E. Paixão, C. M. Dias, P. Nogueira, and J. M. Falcão. 2011. "Air Conditioning and Intrahospital Mortality During the 2003 Heatwave in Portugal: Evidence of a Protective Effect." *Occupational and Environmental Medicine* 68 (3): 218–223. doi:10.1136/oem.2010.058396.

Özgür, L., V. K. Akram, M. Challenger, and O. Dağdeviren. 2018. "An IoT Based Smart Thermostat." In *2018 5th International Conference on Electrical and Electronic Engineering (ICEEE)*, 252–256. IEEE. doi:10.1109/ICEEE2.2018.8391341.

Patz, J., D. Campbell-Lendrum, T. Holloway, and J. Foley. 2002. "Impact of Regional Climate Change on Human Health." *Nature*. 438: 310–317. doi:10.1038/nature04188.

Peng, B., and S.-J. Hsieh. 2017. "Data-Driven Thermal Comfort Prediction with Support Vector Machine." In *Volume 3: Manufacturing Equipment and Systems*, V003T04A044. American Society of Mechanical Engineers, Los Angeles, California, USA.

Porritt, S. M., P. C. Cropper, L. Shao, and C. I. Goodier. 2012. "Ranking of Interventions to Reduce Dwelling Overheating During Heat Waves." *Energy and Buildings* 55: 16–27. doi:10.1016/j.enbuild.2012.01.043.

Prasanna, M. 2014. "A Novel Approach for Optimal Allocation of a Distributed Generator in a Radial Distribution Feeder for Loss Minimization and Tail End Node Voltage Improvement During Peak Load." In *International Transaction of Electrical and Computer Engineers System*. http://pubs.sciepub.com/iteces/2/2/4/iteces-2-2-4.pdf.

Robinson, P. J. 2001. "On the Definition of a Heat Wave." *Journal of Applied Meteorology and Climatology* 40 (4): 762–775. doi:10.1175/1520-0450(2001)040 < 0762:OTDOAH > 2.0.CO;2.

Shan, C., H. Jiawen, J. Wu, A. Zhang, G. Ding, and L. X. Xu. 2020. "Towards Non-Intrusive and High Accuracy Prediction of Personal Thermal Comfort Using a Few Sensitive Physiological Parameters." *Energy and Buildings* 207: 109594. doi:10.1016/j.enbuild.2019.109594.

Simson, R., J. Kurnitski, and M. Maivel. 2017. "Summer Thermal Comfort: Compliance Assessment and Overheating Prevention in New Apartment Buildings in Estonia." *Journal of Building Performance Simulation* 10 (4): 378–391. doi:10.1080/19401493.2016.1248488.

Taylor, M., N. C. Brown, and D. Rim. 2021. "Optimizing Thermal Comfort and Energy Use for Learning Environments." *Energy and Buildings* 248: 111181. doi:10.1016/j.enbuild.2021.111181.

Torriti, J. 2012. "Price-Based Demand Side Management: Assessing the Impacts of Time-of-Use Tariffs on Residential Electricity Demand and Peak Shifting in Northern Italy." *Energy* 44 (1): 576–583. doi:10.1016/j.energy.2012.05.043.

Vandentorren, S., P. Bretin, A. Zeghnoun, L. Mandereau-Bruno, A. Croisier, C. Cochet, J. Ribéron, et al. 2006. "August 2003 Heat Wave in France: Risk Factors for Death of Elderly People Living at Home." *European Journal of Public Health* 16 (6): 583–591. doi:10.1093/eurpub/ckl063.

Ward, D. M. 2013. "The Effect of Weather on Grid Systems and the Reliability of Electricity Supply." *Climatic Change* 121 (1): 103–113. doi:10.1007/s10584-013-0916-z.

Wu, M., H. Li, and H. Qi. 2020. "Using Electroencephalogram to Continuously Discriminate Feelings of Personal Thermal

Comfort Between Uncomfortably Hot and Comfortable Environments." *Indoor Air* 30 (3): 534–543. doi:10.1111/ina.v30.3.

Xu, F. Y., T. Zhang, L. L. Lai, and H. Zhou. 2015. "Shifting Boundary for Price-Based Residential Demand Response and Applications." *Applied Energy* 146: 353–370. doi:10.1016/j.apenergy.2015.02.001.

Yammen, S., S. Tang, and M. K. R. Vennapusa. 2019. "Iot Based Speed Control of Smart Fan." In *2019 Joint International Conference on Digital Arts, Media and Technology with ECTI Northern Section Conference on Electrical, Electronics, Computer and Telecommunications Engineering (ECTI DAMT-NCON)*, 17–20. IEEE. doi:10.1109/ECTI-NCON.2019.8692304.

Yang, Y., T. Nishikawa, and A. E. Motter. 2017. "Small Vulnerable Sets Determine Large Network Cascades in Power Grids." *Science (New York, N.Y.)* 358 (6365): eaan3184. doi:10.1126/science.aan3184.

Yang, B., S. Schiavon, C. Sekhar, D. Cheong, K. W. Tham, and W. W. Nazaroff. 2015. "Cooling Efficiency of a Brushless Direct Current Stand Fan." *Building and Environment* 85: 196–204. doi:10.1016/j.buildenv.2014.11.032.

Yau, Y., and S. Hasbi. 2013. "A Review of Climate Change Impacts on Commercial Buildings and Their Technical Services in the Tropics." *Renewable and Sustainable Energy Reviews* 18: 430–441. doi:10.1016/j.rser.2012.10.035.

Yun, K., R. Luck, P. J. Mago, and H. Cho. 2012. "Building Hourly Thermal Load Prediction Using an Indexed Arx Model." *Energy and Buildings* 54: 225–233. doi:10.1016/j.enbuild.2012.08.007.

Zhao, H.-x., and F. Magoulès. 2012. "A Review on the Prediction of Building Energy Consumption." *Renewable and Sustainable Energy Reviews* 16 (6): 3586–3592. doi:10.1016/j.rser.2012.02.049.

Zhao, Q., Y. Zhao, F. Wang, J. Wang, Y. Jiang, and F. Zhang. 2014. "A Data-Driven Method to Describe the Personalized Dynamic Thermal Comfort in Ordinary Office Environment: From Model to Application." *Building and Environment* 72: 309–318. doi:10.1016/j.buildenv.2013.11.008.